Article

Copolymerization of Ethylene with Polar Monomers: Chain Propagation and Side Reactions. A DFT Theoretical Study Using Zwitterionic Ni(II) and Pd(II) Catalysts

Miklos J. Szabo, Natasha M. Galea, Artur Michalak, Sheng-Yong Yang, Laurent F. Groux, Warren E. Piers, and Tom Ziegler

J. Am. Chem. Soc., **2005**, 127 (42), 14692-14703• DOI: 10.1021/ja052350x • Publication Date (Web): 28 September 2005

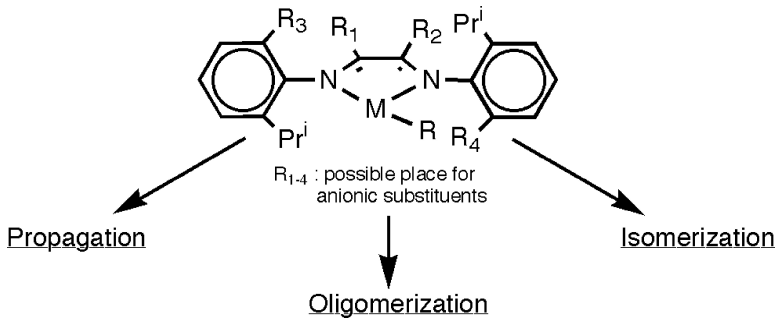

More About This Article

Additional resources and features associated with this article are available within the HTML version:

- Supporting Information
- Links to the 1 articles that cite this article, as of the time of this article download
- Access to high resolution figures
- Links to articles and content related to this article
- Copyright permission to reproduce figures and/or text from this article

View the Full Text HTML

J|A|C|S
ARTICLES
Published on Web 09/28/2005

Copolymerization of Ethylene with Polar Monomers: Chain Propagation and Side Reactions. A DFT Theoretical Study Using Zwitterionic Ni(II) and Pd(II) Catalysts

Miklos J. Szabo,[†] Natasha M. Galea,[†] Artur Michalak,[‡] Sheng-Yong Yang,[†] Laurent F. Groux,[†] Warren E. Piers,[†] and Tom Ziegler*,[†]

Contribution from the Department of Chemistry, University of Calgary, University Drive 2500, Calgary, AB, Canada T2N 1N4, and Department of Theoretical Chemistry, Faculty of Chemistry, Jagiellonian University, R. Ingardena 3, 30-060 Cracow, Poland

Received April 11, 2005; E-mail: ziegler@ucalgary.ca

Abstract: Calculations utilizing anionic substituted derivates of the cationic N^N Ni(II) and Pd(II) diimine Brookhart complex have been carried out on the barriers of ethylene and acrylonitrile insertion into a M− methyl, propyl and CH(CN)Et bond for M = Ni, Pd. The possibility of side reactions such as chelate formation with the polar functionality and oligomerization of the active species after acrylonitrile insertion are explored. The diimine ring system N^N = $-NR''CR_1CR_2NR''$ with R″ = 2,6-C_6H_3(*i*-Pr)$_2$ and R_1,R_2 = Me was functionalized by adding one or two anionic groups (BF_3^-, etc.) in place of *i*-Pr on the aryl rings or by replacing one Me diimine backbone group (R_1) with BH_3^-. The objective of this investigation is computationally to design catalysts for ethylene/acrylonitrile copolymerization that have activities that are comparable to that of the cationic Ni(II) diimine or at least the Pd(II) diimine Brookhart system for ethylene homopolymerization. Complexes that might meet this objective are discussed.

Introduction

Copolymerization of ethylene with polar monomers by late transition metals is a very challenging and active research area.[1,2] Currently, producing polymers involving CH_2═CHX polar monomers is only viable by radical polymerization processes, which are limited in their performance and variability.[3] The existing and very effective coordination polymerization catalysts based on early transition metals[4,5] are very valuable for nonpolar copolymerization. However, early metal catalysts are poisoned by polar groups and thus are unable to copolymerize CH_2═CHX with ethylene.[6]

Late transition metal complexes are more resistant against poisoning. Polar group tolerant bidentate N−O and P−O complexes have been developed by Grubbs[7] and Keim,[8] respectively. The latter type of complexes have further been shown by Drent[9] to copolymerize ethylene and acrylate (Scheme 1). Also, coordination copolymerization of acrylate and vinyl ketones with ethylene has been accomplished by Brookhart[10] with a cationic Pd(II) diimine type catalyst (Scheme 1).

In both experimental[11,12] and theoretical[13h] studies, the cationic Brookhart catalyst was considered to be made even more tolerant toward polar groups by introducing anionic substituents. It should be noted that copolymerization of vinyl chloride with

[†] University of Calgary.
[‡] Jagiellonian University.

(1) (a) Boffa, L. S.; Novak, B. M. *Chem. Rev.* **2000**, *100*, 1479−1493. (b) Gibson, V. C.; Spitzmesser, S. K. *Chem Rev.* **2003**, *103*, 283−316.
(2) (a) Mecking, S. *Coord. Chem. Rev.* **2002**, *203*, 325351. (b) Zuideveld, M. A.; Wehrmann, P.; Röhr, C.; Mecking, S. *Angew. Chem., Int. Ed.* **2004**, *43*, 869−869.
(3) (a) Hagman, J. F.; Crary, J. W. *Encyclopedia of Polymer Science and Engineering*; Mark, H. F.; Bikales, N. W.; Overberger, C. G.; Menges, G.; Kroschwitz, J. I., Eds.; Wiley: New York, 1985; Vol. 1, p 325. (b) Yang, P.; Chan, B. C. K.; Baird, M. C. *Organometallics* **2004**, *23*, 2752−2761.
(4) Hlatky, G. G. *Chem. Rev.* **2000**, *100*, 1347−1376.
(5) Alt, H. G.; Köppl, A. *Chem. Rev.* **2000**, *100*, 1205−1222.
(6) (a) Stockland, R. A., Jr.; Foley, S. R.; Jordan, R. F. *J. Am. Chem. Soc.* **2003**, *125*, 796−809. (b) Stockland, R. A., Jr.; Jordan, R. F. *J. Am. Chem. Soc.* **2000**, *122*, 6315−6316.
(7) (a) Younkin, T. R.; Connor, E. F.; Henderson, J. I.; Friedricj, S. K.; Grubbs, R. H.; Bansleben, D. A. *Science* **2000**, *287*, 460−462. (b) Wang, C.; Friedrich, S.; Younkin, T. R.; Li, R. T.; Grubbs, R. H.; Bansleben, D. A.; Day, M. W. *Organometallics* **1998**, *17*, 3149−3151.
(8) Keim, W.; Kowalt, F. H.; Goddard, R.; Krüger, C. *Angew. Chem., Int. Ed.* **1978**, *17*, 466−467.
(9) (a) Drent, E.; Budzelaar, P. H. M.; Drent, E.; Van Dijk, R.; Van Ginkel, R.; Van Oort, Z. B.; Pugh, R. I. *Chem. Comm.* **2002**, 744−745. (b) Drent, E.; Van Dijk, R.; Van Ginkel, R.; Van Oort, Z. B.; Pugh, R. I. *Chem. Comm.* **2002**, 964−965.
(10) (a) Ittel, S. D.; Johnson, L. K.; Brookhart, M. *Chem. Rev.* **2000**, *100*, 1169−1203. (b) Johnson, L. K.; Killian, C. M.; Brookhart, M. *J. Am. Chem. Soc.* **1995**, *117*, 6414−6415. (c) Killian, C. M.; Tempel, D. J.; Johnson, L. K.; Brookhart, M. *J. Am. Chem. Soc.* **1996**, *118*, 11664−11665. (d) Mecking, S.; Johnson, L. K.; Wang, L.; Brookhart, M. *J. Am. Chem. Soc.* **1998**, *120*, 888−899. (e) Gottfried, A. C.; Brookhart, M. *Macromolecules* **2003**, *36*, 3085−3100. (f) Johnson, L. K.; Mecking, S.; Brookhart, M. *J. Am. Chem. Soc.* **1996**, *118*, 267−268.
(11) (a) Komon, Z. J. A.; Bu, X.; Bazan, G. C. *J. Am. Chem. Soc.* **2000**, *122*, 1830−1831. (b) Komon, Z. J. A.; Bu, X.; Bazan, G. C. *J. Am. Chem. Soc.* **2000**, *122*, 12379−12380. (c) Lee, B. Y.; Bu, X.; Bazan, G. C. *Organometallics* **2001**, *20*, 5425−5431. (d) Kim, Y. H.; Kim, T. H.; Lee, B. Y.; Woodmansee, D.; Bu, X.; Bazan, G. C. *Organometallics* **2002**, *21*, 3082−3084. (e) Komon, Z. J. A.; Diamond, G. M.; Leclerc, M. K.; Murphy, V.; Okazaki, M.; Bazan, G. C. *J. Am. Chem. Soc.* **2002**, *124*, 15280−15285. (f) Shim, C. B.; Kim, Y. H.; Lee, B. Y.; Dong, Y.; Yun, H. *Organometallics* **2003**, *22*, 4272−4280.
(12) (a) Thomas, J. C.; Peters, J. C. *Inorg. Chem.* **2003**, *42*, 5055−5073. (b) Lu, C. C.; Peters, J. C. *J. Am. Chem. Soc.* **2002**, *124*, 5272−5273.
(13) (a) Deubel, D. V.; Ziegler, T. *Organometallics* **2002**, *21*, 1603−1611. (b) Deubel, D. V.; Ziegler, T. *Organometallics* **2002**, *21*, 4432−4441. (c) Michalak, A.; Ziegler, T. *Organometallics* **2001**, *20*, 1521−1532. (d) Michalak, A.; Ziegler, T. *J. Am. Chem. Soc.* **2001**, *123*, 12266−12278. (e) Michalak, A.; Ziegler, T. *Organometallics* **1999**, *18*, 3998−4004. (f) Michalak, A.; Ziegler, T. *Organometallics* **2000**, *19*, 1850−1858. (g) Michalak, A.; Ziegler, T. *Organometallics* **2003**, *22*, 2660−2669. (h) Szabo, M. J.; Jordan, R. F.; Michalak, A.; Piers, W. E.; Weiss, T.; Yang, S.-Y.; Ziegler, T. *Organometallics* **2004**, *23*, 5565−5572.

10.1021/ja052350x CCC: $30.25

Scheme 1. Existing Catalysts for Polar/Nonpolar Copolymerization

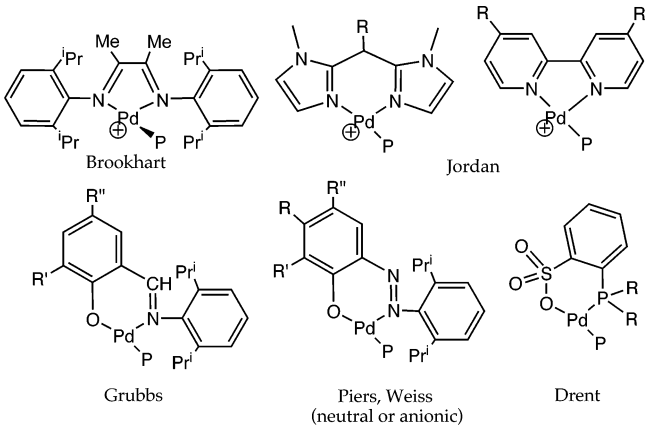

ethylene has met with little success for reasons explained by Jordan.[14] Further, polar copolymerization has been the subject of several theoretical studies.[13,15,16]

A special challenge in polar copolymerization is posed by nitrogen containing monomers such as acrylonitrile (AN) where the tendency toward catalyst poisoning is especially strong. Nevertheless, Piers[17] and Jordan[18] have managed to carry out a single insertion of AN into a Pd(II) alkyl bond, Scheme 1.

The acrylonitrile insertion observed by Piers is viable because the neutral or anionic Pd-salicylaldiminato complex employed was tolerant enough against the N-binding of the polar CN group. This functional group tolerance is made possible because the π-binding is thermodynamically competitive with the N-binding of the acrylonitrile (Scheme 2) as shown theoretically by Deubel and Ziegler.[13a,b] Therefore the π-complex can exist in the reaction mixture and can undergo rapid 2,1 insertion to give an α-cyanoalkyl complex **F**, which can stabilize further in a chelate structure **G**. The general mechanism for the insertion of ethylene and acrylonitrile is shown in Scheme 3.

Deubel and Ziegler[13a,b] first reported that the N-complexation was strongly preferred over the π-complexation for a cationic Brookhart catalyst. Therefore, it is somewhat surprising that Jordan[18] could achieve an acrylonitrile insertion even with a possibly moderately poisoned cationic Pd(II)-N^N complex.

In our previous study we investigated the relative stabilization energies for the coordination of the π and σ functionalities of acrylonitrile and π coordination of ethylene to the metal center of many zwitterionic bulky neutral Ni and Pd diimine Brookhart type complexes in order to explore ways in which to reduce catalyst poisoning in the original cationic Brookhart systems by anionic substitution.[19] It was shown that the introduction of one or two anionic substituents on the backbone of the classical

Scheme 2. π- vs σ-Complexation of Ethylene and Acrylonitrile

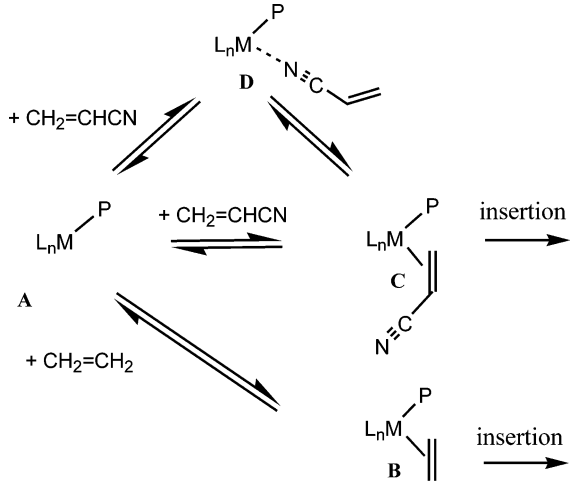

P= growing polymer chain

M= late transition metal, in the present study Ni(II) or Pd(II)

L_n=N–N, N–O, P–P, or other bidentate frameworks

nickel Brookhart catalyst reduces the poisoning, but the N-binding mode is still preferred by 7−11 kcal mol^{-1} over the π-complex formation. A palladium diimine complex substituted on the backbone performs better than the nickel complex.[13h] An even larger reduction in poisoning was found by substituting one or two *i*-Pr groups on the aryl rings with an anionic group, even for a nickel diimine framework. In fact the π-complexation mode becomes favored with the best catalyst candidates.

The objective of the current investigation in the first place is to extend the previous study[19] on poisoning to also include activity by taking a number of promising candidates, **1**−**11** of Scheme 4, with no or modest poisoning and calculate the corresponding insertion barriers for ethylene and AN. Insertion activation energies presented here will further be combined with monomer complexation energies (ethylene or AN) obtained previously[19] in a kinetic scheme[19] that affords relative propagation rates for ethylene and AN insertion. These rates are ultimately used to rank and evaluate the candidates **1**−**11** as copolymerization candidates.

Unfortunately, after the first acrylonitrile insertion Piers'[17] and Jordan's[18] catalysts deactivated because of the side reactions starting from a cyanoalkyl insertion product, Scheme 5. A computational study by Yang et al. has underlined this point.[20] Thus, a good polymerization catalyst must in addition exhibit low affinity toward side reactions involving chelate formation with the polar functionality after insertion or oligomerization of the active species after the acrylonitrile insertion. We have as a second objective studied these possibilities for our best nickel and palladium based candidates (**1**, **9**−**11**), Scheme 4.

Using the previously developed kinetic model[19] for ethylene and acrylonitrile propagation we shall finally examine a few existing Pd(II) complexes, **14** and **15**, that have been shown experimentally to perform a single AN insertion into a palladium carbon bond.[17] We are as a final objective going to compare the few experimental data with the calculated values (**12** and **13** presented in Scheme 6) in order to validate our kinetic model.

(14) (a) Foley, S. R.; Stockland, R. A., Jr.; Shen, H.; Jordan, R. F. *J. Am. Chem. Soc.* **2003**, *125*, 4350−4361. (b) Shen, H.; Jordan, R. F. *Organometallics* **2003**, *22*, 1878−1887.
(15) (a) Philipp, D. M.; Muller, R. P.; Goddard, W. A., III; Storer, J.; McAdon, M.; Mullins, M. *J. Am. Chem. Soc.* **2002**, *124*, 10198−10210. (b) Boone, H. W.; Athey, P. S.; Mullins, M. J.; Philipp, D.; Muller, R.; Goddard, W. A. *J. Am. Chem. Soc.* **2002**, *124*, 8790−8791.
(16) Von Schenck, H.; Stromberg, S.; Zetterberg, K.; Ludwig, M.; Akermark, B.; Svensson, M. *Organometallics* **2001**, *20*, 2813−2819.
(17) Groux, L. F.; Weiss, T.; Reddy, D. N.; Chase, P. A.; Piers, W. A.; Ziegler, T.; Parvez, M.; Benet-Buchholz, J. *J. Am. Chem. Soc.* **2005**, *127*, 1854−1869.
(18) Wu, F.; Foley, S. R.; Burns, C. T.; Jordan, R. *J. Am. Chem. Soc.* **2005**, *127*, 1841−1853.
(19) Szabo, M. J.; Galea, N. M.; Michalak, A.; Yang, S.-Y.; Groux, L. F.; Piers, W. E.; Ziegler, T. *Organometallics* **2005**, *24*, 2147−2156.
(20) Yang, S.-Y.; Szabo, M. J.; Michalak, A.; Weiss, T.; Piers, W. E.; Jordan, R. F.; Ziegler, T. *Organometallics* **2005**, *24*, 1242−1251.

Scheme 3. Insertion of Ethylene and Acrylonitrile into a Metal−Carbon Bond

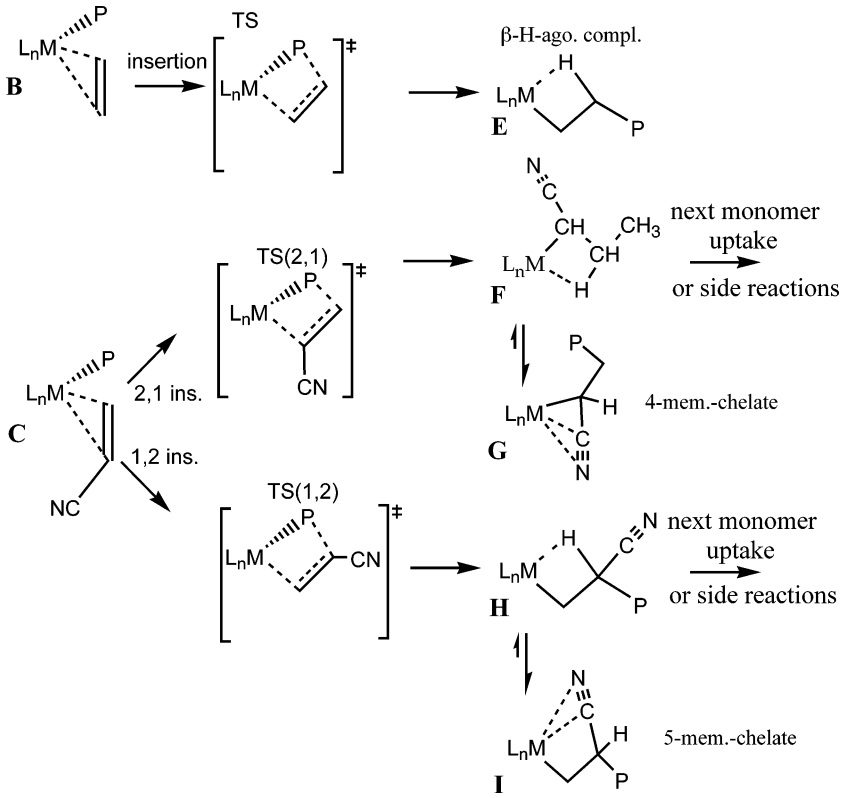

Scheme 4. Neutral and Anionic Diimine Complexes with Anionic Groups and Various Bulky Substituents at the Backbone

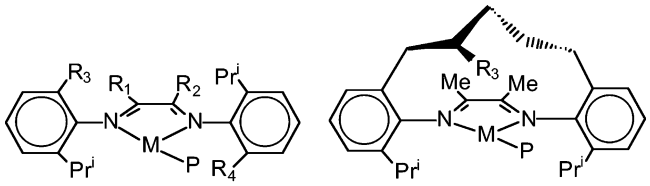

(**0**-**7**,**9**-**11**) (**8**)

ID	M	R_1	R_2	R_3	R_4
0	Ni	Me	Me	Pr^i	Pr^i
1	Ni	Me	Me	BF_3^-	Pr^i
2	Ni	Me	Me	SO_3^-	Pr^i
3	Ni	CF_3	CF_3	BF_3^-	Pr^i
4	Ni	Bu^t	Bu^t	BF_3^-	Pr^i
5	Ni	Bu^t	Bu^t	SO_3^-	Pr^i
6	Ni	Me	Me	BF_3^-	BF_3^-
7	Ni	CF_3	CF_3	BF_3^-	BF_3^-
8	Ni	-	-	β−BF_3^-	-
9	Ni	BH_3^-	Me	Pr^i	Pr^i
10	Pd	Me	Me	BF_3^-	Pr^i
11	Pd	BH_3^-	Me	Pr^i	Pr^i

Computational Details

Molecular geometries have been optimized at the level of gradient-corrected density functional theory using the Becke−Perdew exchange-correlation functional.[21−23] The calculations were carried out with the Amsterdam Density Functional (ADF 2004) program package developed by Baerends et al.[24,25] and vectorized by Ravenek.[26,27] The numerical integration scheme applied for the calculations was developed by te Velde et al.[28] The geometry optimization procedure was based on the method of Versluis and Ziegler.[29] For nickel ($n = 3$) and palladium ($n = 4$) a standard triple-ζ STO basis set, from the ADF database IV, was employed with *n*s, *n*p, *n*d, $(n + 1)$s, $(n + 1)$p treated as valence and the rest as frozen core. For the nonmetal elements a standard double-ζ basis set with one set of polarization functions (ADF database III) was applied, with frozen cores including 1s electrons for B, C, N, O and 1s2s2p for Al.[30,31] Auxiliary[32] s, p, d, f, and g STO functions centered on all nuclei were used to fit the Coulomb and exchange potentials during the SCF process. The reported relative energies include scalar relativistic corrections.[33−35] All structures shown correspond to minimum points on the potential surface, except those prefixed by TS, which represent transition states. Transition states were fully optimized using the algorithm of Banerjee et al.[36,37] starting from the structures obtained by linear transit calculations. No symmetry constraints were used.

(21) Becke, A. *Phys. Rev. A* **1988**, *38*, 3098−3100.
(22) Perdew, J. P. *Phys. Rev. B* **1986**, *34*, 7406−7406.
(23) Perdew, J. P. *Phys. Rev. B* **1986**, *33*, 8822−8824.
(24) Baerends, E. J. Ph.D. Thesis, Free University, Amsterdam, The Netherlands, 1973.
(25) Baerends, E. J.; Ellis, D. E.; Ros, P. *J. Chem. Phys.* **1973**, *2*, 41−51.
(26) Ravenek, W. In *Algorithms and Applications on Vector and Parallel Computers*; te Riele, H. J. J.; Dekker, T. J.; van de Horst, H. A., Eds.; Elsevier: Amsterdam, The Netherlands, 1987.
(27) Boerrigter, P. M.; te Velde, G.; Baerends, E. J. *Int. J. Quantum Chem.* **1988**, *33*, 87−113.
(28) Te Velde, G.; Baerends, E. J. *J. Comput. Phys.* **1992**, *99*, 84−98.
(29) Versluis, L.; Ziegler, T. *J. Chem. Phys.* **1988**, *88*, 322−328.
(30) Snijders, J. G.; Baerends, E. J.; Vernoijs, P. *At. Nucl. Data Tables* **1982**, *26*, 483−509.
(31) Vernoijs, P.; Snijders, J. G.; Baerends, E. J. *Slater Type Basis Functions for the Whole Periodic* System; Internal report (in Dutch); Department of Theoretical Chemistry, Free University: Amsterdam, The Netherlands, 1981.
(32) Krijn, J.; Baerends, E. J. *Fit Functions in the HFS Method*; Internal Report (in Dutch); Department of Theoretical Chemistry, Free University: Amsterdam, The Netherlands, 1984.
(33) Ziegler, T.; Baerends, E. J.; Snijders, J. G.; Ravenek, W.; Tschinke, V. *J. Phys. Chem.* **1989**, 93, 3050−3056.
(34) Snijders, J. G.; Baerends, E. J. *Mol. Phys.* **1978**, *36*, 1789−1804.
(35) Snijders, J. G.; Baerends, E. J.; Ros, P. *Mol. Phys.* **1979**, *38*, 1909−1929.
(36) Banerjee, A.; Adams, N.; Simons, J.; Shepard, R. *J. Phys. Chem.* **1985**, *89*, 52−57.
(37) Fan, L.; Ziegler, T. *J. Chem. Phys.* **1990**, *92*, 3645−3652.

Scheme 5. Possible Reactions after a Prior 2,1 Acrylonitrile Insertion

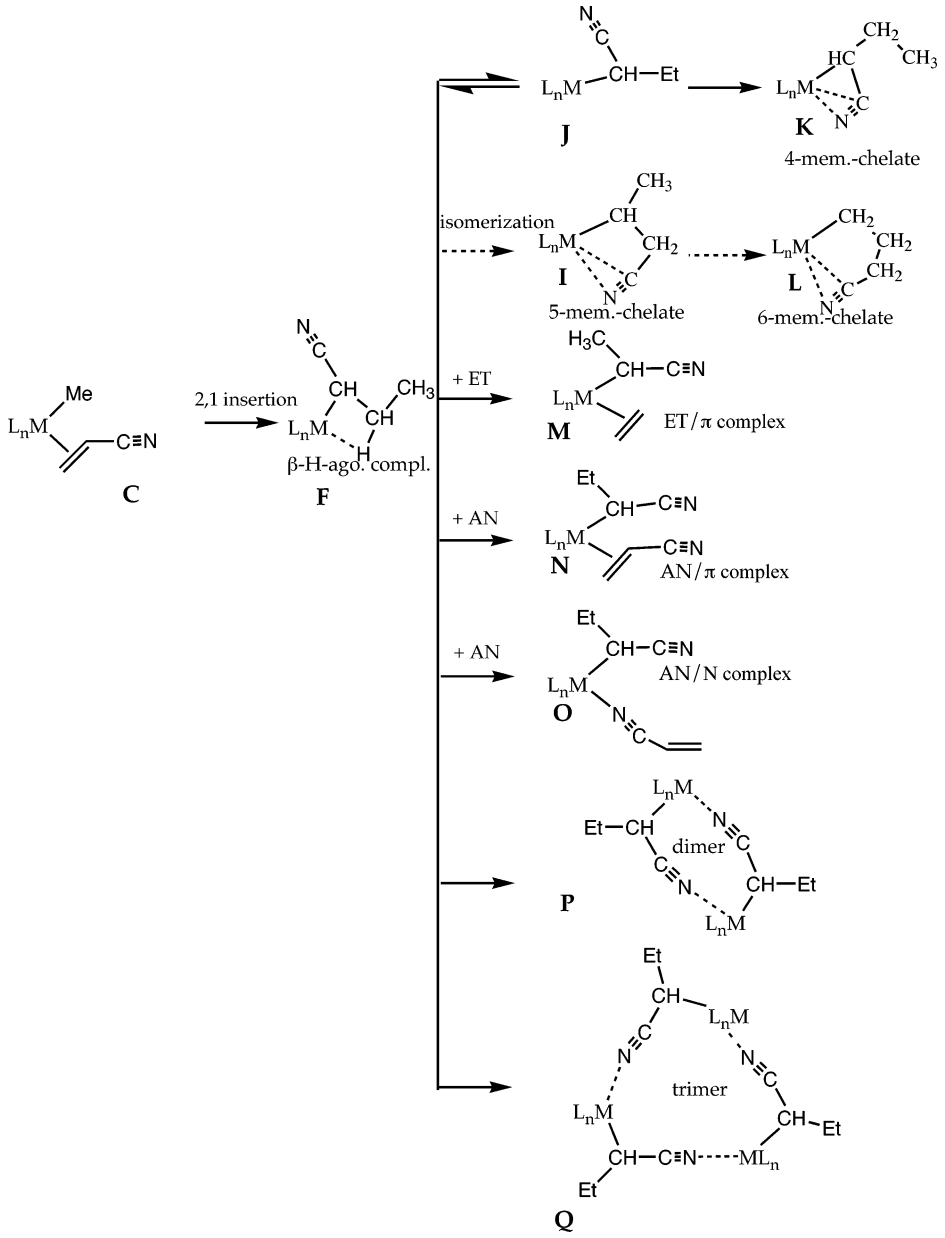

Scheme 6. Different Polymerization Catalysts

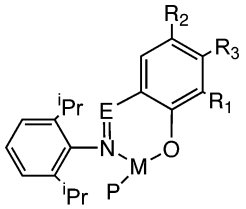

ID	M	E	R_1	R_2	R_3
12	Pd	N	^{t}Bu	^{t}Bu	H
13	Pd	N	^{t}Bu	^{t}Bu	BH_3^-
14	Pd	CH	^{t}Bu	H	H
15	Pd	CH	^{t}Bu	BF_3^-	H

The combined DFT and molecular mechanics calculations were performed using the quantum mechanics/molecular mechanics (QM/MM) implementation in the ADF program.[38] An augmented Sybyl molecular mechanics force field[39] was utilized to describe the molecular mechanics potential, which includes van der Waals parameters from the UFF forces field[40] for nickel, palladium, and boron.

For backbone substituted zwitterionic complexes a specific partitioning format was applied as illustrated in Scheme 7A. The quantum mechanical part contains the generic nickel or palladium diimine complex including the anionic substituent. The rest of the molecule including the (*i*-Pr)$_2$Ph ring and the Me group on the backbone is part of the molecular mechanics region. A ratio, α, of 1.40 and 1.34 was employed for the N(sp^2)−C(aryl) and C(sp^2)−C(sp^3) link bonds, respectively, in the nickel complexes of ligand **9**, to reproduce the average experimental bond distances[13g] for related compounds. For the palladium complexes of ligand **11**, a ratio, α, of 1.321 and 1.34 was adopted from previous work[13h] for the N(sp^2)−C(aryl) and C(sp^2)−C(sp^3) links, respectively.

The partitioning scheme, shown in Scheme 7B, was used to study the possible ring structures **P** and **Q** produced by oligomerization of the 2,1 acrylonitrile insertion products **F** or **J** containing an α-CN group.

(38) Woo, T. K.; Cavallo, L.; Ziegler, T. *Theor. Chem. Acc.* **1998**, *100*, 307−313.
(39) Clark, M.; Cramer, R. D., III; van Opdenbosch, N. *J. Comput. Chem.* **1989**, *10*, 982−1012.
(40) Rappe, A. K.; Casewit, C. J.; Colwell, K. S.; Goddard, W. A., III.; Skiff, W. M. *J. Am. Chem. Soc.* **1992**, *114*, 10024−10035.

Scheme 7. Partitioning of the System into Molecular Mechanics (in Dotted Area) and Quantum Mechanics Regions

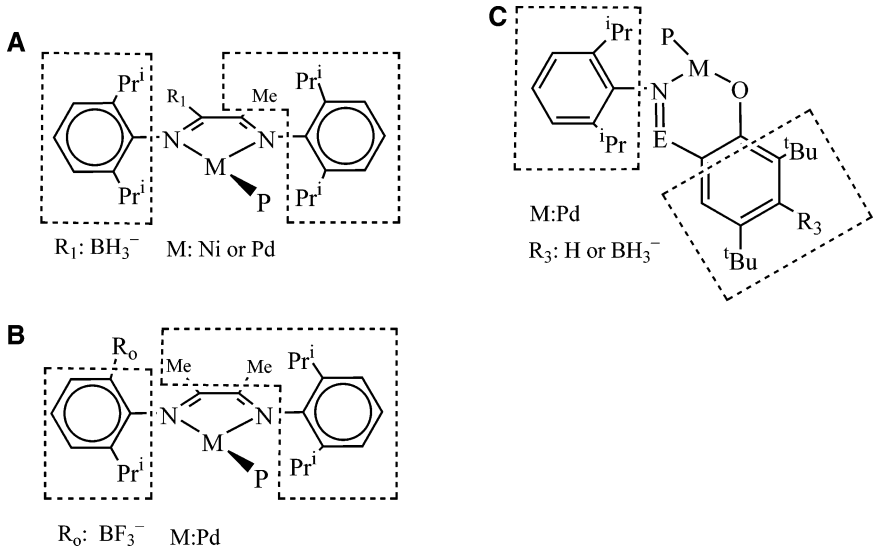

A disconnected QM unit was applied to mimic the effect of the ortho-phenyl anionic BF_3^- group. Based on quantum chemical calculations for complexes **1** and **10**, an α=1.30 link parameter was employed to reproduce the B−C(aryl) bond length in the QM/MM model. Hydrogens were used as capping atoms. This hybrid model successfully (within 1 kcal mol^{-1}) reproduced the difference between the π- and N-complexation energy, obtained from a calculation from which the full **1**/**E** structure was treated by quantum chemical method.

Scheme 7C shows the partitioning of the complexes **12**−**13** studied by Yang and co-workers. In this previous study,[20] a ratio, α, of 1.328 and 1.420 was adopted for the N(aryl) and C(aryl)−C(R) link bonds, respectively, to reproduce the average experimental bond distances in related neutral Pd−N^O compounds.

The solvation energies based on gas-phase geometries were calculated by the conductor-like screening model (COSMO)[41] with a dielectric constant of 2.379 corresponding to toluene as the solvent. The radii used for the atoms (in Å) were as follows: C, 2.0; H, 1.18; B, 1.15; N, 1.5; F, 1.2; Ni, 2.5. We have tested the effect of the solvent for the zwitterionic neutral complex **1**. The energetics of the key reaction steps using the solvation model only differ by a maximum of 2.4 kcal mol^{-1} from the gas phase results. Therefore we expect only a minor solvation effect for the zwitterionic Ni-neutral complexes. The energetics discussed below are missing zero-point vibrational energy and entropic corrections, since it was impractical to perform a vibrational analysis on systems of the size considered here. We expect these corrections to be on the order of ±2−3 kcal/mol.

Kinetic Model for Propagation of Ethylene and Acrylonitrile by Coordination Polymerization. The mechanism for ethylene and acrylonitrile (coordination) copolymerization is shown in Scheme 8. Both ethylene and acrylonitrile can form a π-complex with the catalytically active species in a reversible step. Acrylonitrile can in addition form an N-complex through its CN functional group. Additionally, the N-complex of acrylonitrile is able to isomerize to a π-complex, without dissociating from the catalyst. Once ethylene or acrylonitrile is π-coordinated it can insert into the metal−alkyl bond forming a new catalytically active species. This mechanism is analogous to that found for Michaelis−Menten enzyme catalyzed reactions, except that the insertion product is a catalytically active species which is able to uptake the next monomer to repeat the catalytic cycle.[42]

The expression for the initial rate of ethylene chain propagation (k_{ET}) according to the mechanism illustrated at the top part of Scheme 8 is

Scheme 8. Mechanism of the Chain Propagation for Ethylene and Acrylonitrile[a]

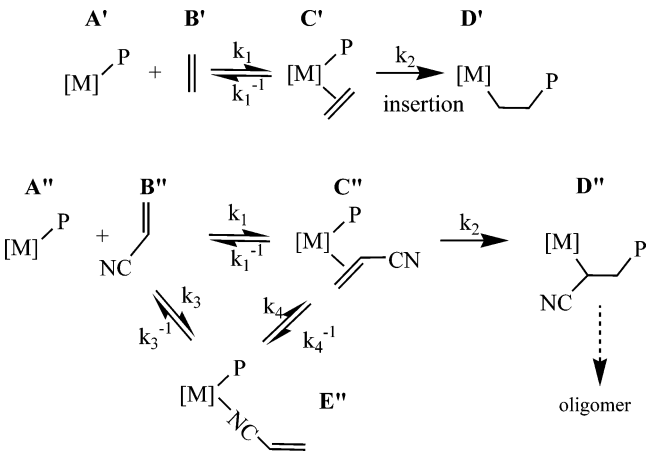

[a] The initial rate of the product formation is expressed in terms of the elementary reaction rates, the initial catalyst concentration A_0, and initial monomer concentration B'_0 and B''_0.

given in eq 1. Here use has been made of the mass balance $[A'] = A_0 - [C']$, where A_0 is the initial catalyst concentration and B'_0 is the initial monomer concentration.[19]

$$k_{ET} = \frac{k_2 k_1 A_0 B'_0}{k_1 B'_0 + k_1^{-1} + k_2} \tag{1}$$

The expression for the rate of acrylonitrile chain propagation (k_{AN}) according to Scheme 8 is more complex, as can be seen in eq 2, due to the two possible binding modes of acrylonitrile and the $\pi-\sigma$ interconversion.

$$k_{AN} = \frac{k_2\left[(k_1 A_0 B_0'') - \dfrac{k_3 B_0'' A_0 (k_1 B_0'' - k_4)}{k_3 B_0'' + k_3^{-1} + k_4}\right]}{k_1 B_0'' + k_1^{-1} + k_2 + k_4^{-1} - \dfrac{(k_3 B_0'' - k_4^{-1})(k_1 B_0'' - k_4)}{k_3 B_0'' + k_3^{-1} + k_4}} \tag{2}$$

The efficiency of propagation of any late transition metal catalyst candidates can be characterized by calculating the propagation rate k_{rel} relative to an internal standard. For ethylene propagation

(41) Pye, C. C.; Ziegler, T. *Theor. Chem. Acta* **1999** *101*, 396−408.
(42) Peuckert, M.; Keim, W. *Organometallics* **1983**, *2*, 594−597.

k_{rel} is defined by eq 3.

$$k_{rel} = k^0_{ET}/k_{ET} \quad (3)$$

As a reference reaction rate k^0_{ET} we choose the original cationic nickel based Brookhart catalyst. On the other hand k_{ET} is the rate of ethylene propagation for a particular catalyst with rate constants k_1, k_1^{-1} and k_2. For acrylonitrile propagation, similarly, we use the same internal standard k^0_{ET} and we define the relative rate for the acrylonitrile propagation k'_{rel} according to eq 4, where k_{AN} is calculated based on eq 2.

$$k'_{rel} = k^0_{ET}/k_{AN} \quad (4)$$

The relative ethylene and polar monomer propagation rates k_{rel} and k'_{rel} are inversely proportional to the corresponding actual rates of monomer chain propagation k_{ET} and k_{AN}, respectively. An increase in the relative monomer propagation rates (k_{rel} and k'_{rel}) demonstrates a decrease in the actual monomer propagation rates (k_{ET} and k_{AN}) and, therefore, a decrease in the activity of the catalyst. This increase/decrease in activity is always relative to the internal standard (k^0_{ET}).

Reaction rate constants k_1, k_1^{-1}, k_2, k_3, k_3^{-1}, k_4, and k_4^{-1}, corresponding to the elementary steps shown in Scheme 8 and appearing in eqs 1 and 2, have been calculated by the standard Eyring equation for a given temperature $T = 263$ K and $p = 1$ bar. The concentration of ethylene is 0.23 mol dm^{-3} under these conditions,[43] and we used the same approximate value for acrylonitrile. Since the concentrations of the monomers are much higher than the concentration of the catalyst we also assume that the olefin concentrations have the constant values B_0' and B_0'', respectively. Molecular dynamics simulations on the Brookhart catalyst have shown that the values of the olefin uptake rates, k_1 and k_3, are determined by an entropic uptake barrier of ~9 kcal mol^{-1} due to loss in the rotational and translational degrees of freedom when the monomer is captured.[44] Furthermore, for the barrier of the interconversion of π and σ acrylonitrile complexes, we use an estimate value $\Delta E_4^{\ddagger} = 25$ kcal mol^{-1} in all systems based on the cationic Brookhart catalyst.

From our kinetic model, which has already been explained in detail in the first part of our studies,[19] we can formulate the prerequisite for an ideal catalyst candidate, which might be able to copolymerize ethylene and acrylonitrile.

(i) A good ethylene propagating polymerization catalyst should have a low barrier of insertion and a strong π-complexation, preferably $\Delta E_\pi < -10$ kcal mol^{-1}.

(ii) Polar monomer incorporation into the polymer chain is only viable if the catalyst is tolerant against the poisoning effect of the polar functionality. However, it must also have a low monomer insertion barrier and a π-complexation energy between $\Delta E_\pi > -20$ and $\Delta E_\pi < -5$ kcal mol^{-1}.

(iii) The overall propagation rate of acrylonitrile should be close to the corresponding propagation rate of ethylene.

(iv) Finally, in addition to conditions (i)−(iii), a good polymerization catalyst should have a low affinity toward other side reactions such as chelate formation with the polar functionality after insertion or oligomerization of the active species after the acrylonitrile insertion; see Scheme 5. We have also studied these possibilities for our best candidates, which were chosen based on conditions (i)−(iii).

Results and Discussion

Based on the kinetic models for ethylene and acrylonitrile propagation we have formulated the prerequisites for an ideal catalyst candidate under points (i)−(iv). The ideal catalyst should have the same ethylene polymerization activity as cationic nickel or palladium based Brookhart systems, in addition to the ability to integrate $-CH_2CH(CN)-$ units into the polymer chain. The first challenging problem in ethylene/acrylonitrile copolymerization is to promote π-complexation over N-coordination in order to avoid catalyst poisoning. Ways in which to reduce poisoning has already been addressed in a previous study.[19] It was further shown in the same investigation that the overall rate of propagation depends not only on the internal insertion barrier as well as catalyst poisoning but also on the ability to form a stable π-complex after the monomer uptake. The previously defined relative reaction rates incorporate all these factors; therefore $\log(k_{rel})$ and $\log(k'_{rel})$ are probably the best indexes for a ranking of different prospective ethylene/AN copolymerization catalysts.

We will study the insertion of ethylene and acrylonitrile into three different types of M−P metal alkyl bonds, where P = methyl, propyl, and α-cyano-propyl groups. Here P = Me models the insertion, whereas P = propyl and P = α-cyano-propyl models propagation after subsequent ethylene and AN insertions, respectively. Table 1 displays the absolute barrier ($\Delta E^{\ddagger}_{ab}$) for the ethylene and acrylonitrile insertion with respect to the separated alkyl complex and a free monomer. Internal barriers ($\Delta E^{\ddagger}_{in}$) are also shown with respect to the energy of the π-complex. It should be mentioned that in Tables 1 and 2 we only tabulate the transition state energies for the lowest energy insertion pathway for each system. For many neutral systems, the anionic substitution reduces the C2 symmetry of the original diimine complex to C1, thus introducing cis−trans isomerism. In Scheme 9, we sketch the transition states for both the cis and trans pathways. We define the terms "trans" or "cis" according to the position of the alkyl group in the square planar geometry with respect to the BF_3^- substituent. For acrylonitrile insertions the trans pathway is favored over the cis mechanism. However in the case of ethylene insertion the difference between the two insertion pathways is negligible. Further, since the π-complex also prefers a cis conformation, no isomerization is required before insertion.

The log of the calculated relative rates, $\log(k_{rel})$ and $\log(k'_{rel})$, as defined in eqs 1−4 are given in Table 2 for the systems **0**−**11**. Graphical representation of the log of the relative rate k_{rel} with respect to ethylene insertion into an M−propyl bond is demonstrated for catalysts **0**−**11**, along with the respective π-complexation energies, in Figure 1. In the cationic Ni(II)-based Brookhart catalyst (**0**) $\log(k'_{rel})$ of acrylonitrile (AN) is some 18 times larger than $\log(k_{rel})$ for ethylene. As a consequence AN propagation is 10^{18} times slower than ethylene propagation. The primary reason for this is catalyst poisoning due to a strong Ni−NC bond that prevents coordination of AN through its C=C double bond as a first step toward insertion.

The objective of anionic substitution is to reduce the poisoning and thus enhance the rate of AN propagation without lowering significantly the activity of the catalyst toward ethylene propagation. A good candidate for ethylene/acrylonitrile insertion should have the same affinity toward ethylene and AN, and an activity comparable to that of the cationic Ni(II)-based Brookhart catalyst (**0**) with $\log(k_{rel}) = 0$ or at the least its Pd(II)-based homologue with $\log(k_{rel}) = 2$. That is, $k_{rel} \approx k'_{rel}$ and $\log(k_{rel})$, $\log(k'_{rel}) < 2$. This is best achieved, for AN propagation, when $k_2 > k_4^{-1}$, and therefore the monomer insertion

(43) Waters, J. A.; Mortimer, G. A.; Clements, H. E. *J. Chem. Eng. Data* **1970**, *15*, 174−176.
(44) Woo, T. K.; Blöchl, P. E.; Ziegler. T. *J. Phys. Chem. A* **2000**, *104*, 121−129.

Table 1. Absolute ($\Delta E^{\ddagger}_{ab}$, kcal mol^{-1}) and Internal ($\Delta E^{\ddagger}_{in}$, kcal mol^{-1}) Barriers for Ethylene and Acrylonitrile Insertion Catalyzed by the Brookhart Complex and Its Derivatives

						ET		AN	
ID	[M]	R_3[a]	R_4[a]	R_1, R_2[a]	P[a]	$\Delta E^{\ddagger}_{ab}$[b]	$\Delta E^{\ddagger}_{in}$[c]	$\Delta E^{\ddagger}_{ab}$[b]	$\Delta E^{\ddagger}_{in}$[c]
0	Ni	Pr^i	Pr^i	Me	Pr^n	2.4	14.5	2.4	14.5
1	Ni	BF_3^-	Pr^i	Me	Me	5.8	19.5	2.9	18.7
					Pr^n	7.4	19.9	4.2	20.5
					CH(CN)Et	4.6	20.1	5.8	23.8
2	Ni	SO_3^-	Pr^i	Me	Me	9.9	20.8	7.0	21.9
					Pr^n	12.1	22.1	12.1	22.1
					CH(CN)Et	7.9	21.2	11.0	28.2
3	Ni	BF_3^-	Pr^i	CF_3	Me	7.1	17.0	6.9	16.9
					Pr^n	8.3	18.9	6.4	17.6
					CH(CN)Et	12.2	16.0		
4	Ni	BF_3^-	Pr^i	Bu^t	Me	11.9	15.3	8.7	13.3
					Pr^n	9.5	12.2	8.3	15.1
					CH(CN)Et	10.2	14.8		
5	Ni	SO_3^-	Pr^i	Bu^t	Me	20.4	20.3	18.5	20.5
					Pr^n	19.3	20.2	16.3	20.8
					CH(CN)Et	14.2	18.0		
6	Ni	BF_3^-	BF_3^-	Me	Me	7.1	17.0	6.9	16.9
					Pr^n	8.3	18.9	6.4	17.6
					CH(CN)Et	12.2	16.0		
7	Ni	BF_3^-	BF_3^-	CF_3	Me	11.9	15.3	8.7	13.3
					Pr^n	9.5	12.2	8.3	15.1
					CH(CN)Et	10.2	14.8		
8	Ni (bridge structure)	β-BF_3^-			Me	−0.6	18.3	−1.2	20.4
					Pr^n	9.7	19.2	−1.3	20.1
					CH(CN)Et	−2.1	18.2		
9	Ni	Pr^i	BH_3^-	Me	Me	−13.0	16.3	−15.4	14.8
					Pr^n	2.2	14.6	−0.6	13.1
					CH(CN)Et	7.7	20.6		
10	Pd	BF_3^-	Pr^i	Me	Me	2.3	20.8	0.9	20.0
					Pr^n	3.5	20.6	0.6	19.1
					CH(CN)Et	4.1	23.9		
11	Pd	Pr^i	BH_3^-	Me	Me	−10.7	21.4	−12.9	19.9
					Pr^n	3.8	21.4	1.0	21.8
					CH(CN)Et	5.7	26.5		

[a] For numbering of groups see Scheme 4. [b] $\Delta E^{\ddagger}_{ab}$ is the lowest insertion barrier relative to the alkyl complex and the free monomer. See Scheme 9 and text. [c] $\Delta E^{\ddagger}_{in}$ is the lowest internal barrier of insertion relative to the trans π-complex.

barrier is lower in energy than the isomerization barrier minus the poisoning of the system ($\Delta E^{\ddagger}_{in} < \Delta E_4^{\ddagger} - P$).

Neutral Ni(II)-Based Aryl Substituted BF_3^- and SO_3^- Systems. We shall start by discussing two candidates as anionic substituents, namely BF_3^- and SO_3^-. The first single substitution with BF_3^- and SO_3^- will be at the ortho position of one of the aryl rings since a previous study[19] has shown that anionic groups in this position considerably reduce catalyst poisoning by AN.

Considering first ethylene insertion into the Ni−P bonds (P = methyl, propyl, and α-cyano-propyl), we note that log(k_{rel}) has increased by factors of roughly 5 (**1**) and 6 (**2**), respectively, compared to **0**, Table 2. The reduction in activity is partially due to larger insertion barriers, Table 1, and they are also caused by a reduction in the π-complexation energies[19] as ethylene has to disrupt the Ni−BF_3 and Ni−SO_3 interactions. In addition ethylene will suffer some steric destabilization from the anionic groups after the π-complex is formed. The reduction in the π-complexation energy will increase k_1^{-1} and thus reduce k_{Et}; see eq 1. As a consequence k_{rel} of eq 3 will increase. The increase in k_{rel} is most noticeable for the bulkier anionic group SO_3^-.

Turning next to the insertion of AN into the Ni−Me and Ni−Pr bonds, we generally note hardly any change in log(k'_{rel}) for AN compared to log(k_{rel}) in the case of ethylene, Table 2. This is in contrast to compound **0** where log(k'_{rel}) is a factor of 18 larger than log(k_{rel}). This improvement is not so much due to a reduction in the insertion barriers of **1** and **2** compared to **0** as in the destabilization of the AN σ-complex. The destabilization comes from the interaction between the negative substituent and the negative charge on the nitrogen group of AN. A reduction in the σ-complexation energy (and catalyst poisoning) will increase k_3^{-1} (Scheme 8) in eq 2 and thus k_{AN} of eq 2. The result is the desired decrease in k'_{rel}. We note as a further bonus that double AN insertion has a lower propagation rate than double ethylene propagation or alternating Et/AN propagation. This is an advantage if the target is polymers with 10−20% AN incorporations.

Finally, as for ethylene insertion, the AN propagation activity is seen to be lower for SO_3^- compared to BF_3^-. This can again be attributed to the larger steric bulk of SO_3^-.

Anionic Aryl Substitution with Me, CF_3, and *t*-Bu Backbone Substituents. We shall next expand on the motif with one anionic substitution in the ortho position of an aryl ring by

Table 2. Log of the Relative Reaction Rates ($\log(k_{rel})$ and $\log(K'_{rel})$) for the Brookhart System and Its Derivatives

ID	[M]	R_3[a]	R_4[a]	R_1[a]	R_2[a]	P[a]	ET $\log(k_{rel})$[b]	AN $\log(K'_{rel})$[c]	average $\log(k_{Arel})$[d]
0	Ni	Pr^i	Pr^i	Me	Me	Pr^n	0.0	18.0	
1	Ni	BF_3^-	Pr^i	Me	Me	Me	4.2	4.6	4.8
						Pr^n	4.5	6.0	
						CH(CN)Et	4.7	12.6	
2	Ni	SO_3^-	Pr^i	Me	Me	Me	5.3	6.2	6.0
						Pr^n	6.5	6.3	
						CH(CN)Et	5.6	12.6	
3	Ni	BF_3^-	Pr^i	CF_3	CF_3	Me	2.3	6.5	5.0
						Pr^n	3.8	6.2	
						CH(CN)Et	6.2		
4	Ni	BF_3^-	Pr^i	Bu^t	Bu^t	Me	6.0	3.3	4.2
						Pr^n	4.0	3.0	
						CH(CN)Et	4.6		
5	Ni	SO_3^-	Pr^i	Bu^t	Bu^t	Me	13.1	11.5	12.0
						Pr^n	12.1	9.6	
						CH(CN)Et	13.5		
6	Ni	BF_3^-	BF_3^-	Me	Me	Me	2.9	3.3	3.9
						Pr^n	3.9	2.3	
						CH(CN)Et	6.8		
7	Ni	BF_3^-	BF_3^-	CF_3	CF_3	Me	1.9	2.8	4.1
						Pr^n	2.0	4.2	
						CH(CN)Et	9.7		
8	Ni	β-BF_3^- (bridge structure)				Me	3.2	8.8	6.8
						Pr^n	4.4	8.7	
						CH(CN)Et	8.6		
9	Ni	Pr^i	Pr^i	BH_3^-	Me	Me	1.5	8.5	4.5
						Pr^n	0.1	7.4	
						CH(CN)Et	5.1		
10	Pd	BF_3^-	Pr^i	Me	Me	Me	5.3	4.7	5.4
						Pr^n	5.1	4.4	
						CH(CN)Et	7.7		
11	Pd	Pr^i	Pr^i	BH_3^-	Me	Me	5.8	8.4	7.3
						Pr^n	5.8	6.5	
						CH(CN)Et	10.0		

[a] For numbering of groups see Scheme 4. [b] Ethylene propagation rate relative to the internal standard, complex **0**, using eq 3. [c] Acrylonitrile propagation rate relative to the internal standard, complex **0**, using eq 4. [d] Average relative propagation rate with respect to ethylene insertion (k_{rel}) into the M−P bond, where P= Me, Pr^n and CH(CN)Et, and acrylonitrile insertion (k'_{rel}) into the M−P bond, where P= Me and Pr^n.

exploring how the corresponding activities are changed by steric and electronic modifications of the diimine backbone. To this end the two methyl groups on the backbone will be replaced by the bulky and more electron-withdrawing CF_3 substituents or with the even more bulky and electron donating Bu^t groups.

Starting first with BF_3^- and introducing the steric backbone substituents CF_3 (**3**) and Bu^t (**4**) will reduce the monomer complexation energies,[19] especially for Bu^t, as the aryl groups are pushed forward toward the monomer. By itself this should lead to a reduction in both the ethylene and the AN propagation rate; however, this effect is compensated by a reduction in the insertion barriers (Table 1). Comparing the backbone substituent CF_3 (**1**,**3**), the propagation activities for ethylene insertion into a Ni−Me and Ni−Pr bond increase due to the reduction in the insertion barriers. This general increase in the propagation rate of ethylene is offset by a decrease in the remaining activities. The decrease in the activity of ethylene insertion into a Ni−CH(CN)Et bond is due to substantial destabilization of the π-complex caused by greater steric interaction between the monomer and the aryl rings. The decrease in the activity of AN is due to the increased poisoning of the system, as well as the destabilization of the monomer complexation energies. Considering the backbone substituent Bu^t (**1**,**4**), all monomer insertions cause an increase in activity due to a considerable reduction in the insertion barriers. The only exception is ethylene insertion into the Ni−Me bond, where a decrease in activity is caused by a very destabilized π-complex (<-5 kcal mol^{-1}) coupled with a greater insertion barrier (>15 kcal mol^{-1}). As a result, generally, the activity decreases very slightly in going from **1** to **3**, while it increases in going from **1** to **4**, Table 2.

For the bulkier anionic group SO_3^- we have only considered the substitution from methyl (**2**) to Bu^t (**5**). This substitution has hardly any influence on the insertion barriers, Table 1. However, it considerably reduces the π-complexation energies[19] and thus the propagation activities, Table 2.

Anionic Ni Aryl BF_3^- Substituted Systems. The promising results from a single anionic BF_3^- substitution on one ring led us to consider an additional BF_3^- substitution on the other aryl ring. The performance of the resulting anionic complexes **6** and **7** with, respectively, Me and CF_3 at the backbone is compared to that of the corresponding monosubstituted neutral complexes **1** and **3** in Table 2.

Scheme 9. Schematic Representation of the Transition States of Cis and Trans Insertion Pathways for Ethylene and Acrylonitrile Insertion[a]

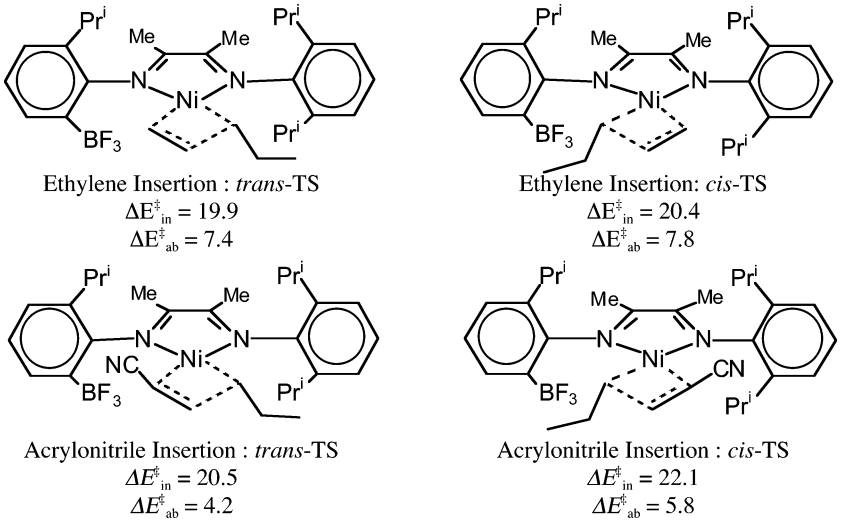

[a] The internal barriers ($\Delta E^{\ddagger}_{in}$, kcal mol^{-1}) are with respect to the energy of the trans π-complex. The absolute barriers ($\Delta E^{\ddagger}_{ab}$, kcal mol^{-1}) are with respect to the separated alkyl complex and the free monomer.

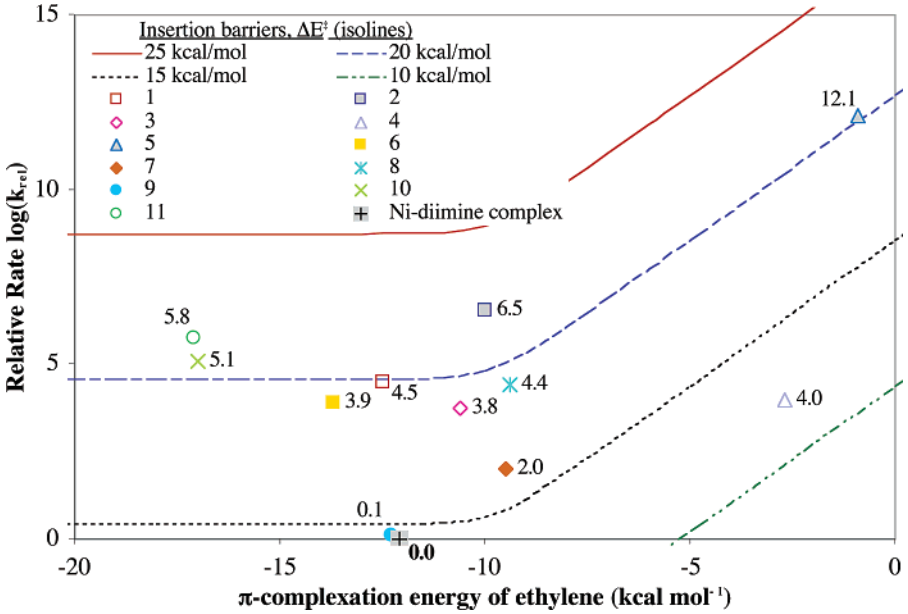

Figure 1. Log of the relative rate ($k_{rel} = k^0_{ET}/k_{ET}$) for ethylene propagation into a propyl chain as a function of the ethylene complexation energy (ΔE_π) for different internal insertion barriers ($\Delta E^{\ddagger}$). k_{ET} is the rate of ethylene propagation into a propyl chain for each catalyst and k^0_{ET} is the rate of ethylene propagation for the original Ni(II) Brookhart catalyst according to eq 1.

We notice a considerable increase in activity in going to the double substituted species **6** and **7**. In fact **6** is our best Ni(II)-based catalyst. Both **6** and **7** are more active for insertion into the Ni−Me and Ni−Pr bonds, whereas **1** and **3** have the highest activity with respect to Ni−CH(CN)Et insertion. In both cases the increased activity is due to lower insertion barriers. A more substantial increase in activity is apparent for AN insertion, compared to ethylene insertion.

Neutral Ni Substituted Systems with Bridge Structure. So far in this investigation, the anionic BF_3^- substituent has been positioned on the ortho carbon of the aryl ring. An alternative possibility is to position the BF_3^- group directly above the metal on an alkyl chain consisting of five carbon atoms that connects the two aryl rings from ortho to ortho position. Based on complexation energy data and catalyst poisoning, the optimum position of the anionic BF_3^- group on the alkyl chain is at the β-carbon,[19] as in complex **8**.

In comparing **8** with **1** we note that **8** is less active with respect to AN insertion due to an increase in catalyst poisoning and a decrease in π-complexation energy.[19] A decrease in π-complexation[19] is also making **8** less active with respect to ethylene insertion into the Ni−CH(CN)Et bonds. It would seem that the motif contained in **8** is less effective than the simple BF_3^- substitution at the ortho position of the aryl rings.

Anionic Substitution at the Diimine Backbone. The final substitution motif we shall consider here has the Me group on the backbone replaced by BH_3^-, **9**. The BH_3^- group in **9** cannot interact directly with the metal center. It can, however, donate electron density to nickel with the result that π-complexation is enhanced through increased metal to ligand π back-donation.

Table 3. Complexation Energies of Compounds **9**−**11**

ID	[M]	R_3[a]	R_4[a]	R_1[a]	R_2[a]	P[a]	ET/π[b]	AN/π[c]	AN/σ[d]	AN($\pi-\sigma$)[e]
9	Ni	Pr^i	Pr^i	BH_3^-	Me	Me	−29.3	−30.2	−38.6	8.4
						Pr^n	−12.3	−13.7	−23.3	9.6
						CH(CN)Et	−12.9	−12.2	−25.4	13.2
10	Pd	BF_3^-	Pr^i	Me	Me	Me	−18.5	−19.1	−18.5	−0.6
						Pr^n	−17.0	−18.5	−18.8	0.2
						CH(CN)Et	−19.7	−19.1	−22.8	3.6
11	Pd	Pr^i	Pr^i	BH_3^-	Me	Me	−32.1	−32.8	−33.7	0.9
						Pr^n	−17.1	−20.6	−20.8	0.2
						CH(CN)Et	−20.8	−21.2	−23.7	2.7

[a] For numbering of groups see Scheme 4. [b] Monomer binding energies for ethylene π-complexes. [c] Monomer binding energies for acrylonitrile π-complexes. [d] Monomer binding energies for acrylonitrile σ-complexes. [e] Poisoning of the CN group, $\Delta E_\pi - \Delta E_\sigma$.

Thus π-complexation in **9** is somewhat stronger than that in **0** and considerably stronger than that in **1**−**8** where the anionic group is on the aryl ring.[19] On the other hand AN σ-bonding is reduced in strength compared to **0** as one might hope for due to the increased electron density on nickel, still **9** has a residual preference for σ- rather than π-complexation to AN of 8.4 kcal mol^{-1} (Table 3).[19]

Turning next to the insertion barriers, Table 1, we note that insertion of ethylene generally has a higher activation energy, while AN has a lower activation energy for **9** compared to **1**. In the final analysis **9** is the most active of the investigated Ni-based catalysts (**1**−**9**) for ethylene insertion, Table 2. On the other hand, **9** is not as good for AN insertion as the best among the aryl substituted catalysts (e.g., **4**, **6**, and **7**) due to the residual poisoning of 8.4 kcal mol^{-1}.

Comparing Theoretical and Experimental Data. A Validation of the Kinetic Model. A previous theoretical investigation carried out by Yang et al.[20] studied ethylene and acrylonitrile insertion into an M−methyl or M−CH(CN)Et bond in the neutral (**12**) and anionic (**13**) Grubbs type Pd−N^O catalysts. A very similar neutral and anionic catalyst (**14**,**15**) was investigated experimentally by Piers,[17] in a study on the activity of acrylonitrile insertion into an M−methyl bond. Piers determined experimentally that propagation using an anionic catalyst was 1.6 times faster than propagation using a neutral catalyst for insertion of AN into the Pd−Me bond. Based on the complexation data and insertion barriers calculated by Yang, the kinetic model employed throughout this work affords the absolute relative rate of reaction (k'_{rel}) for acrylonitrile insertion into a methyl chain to be 2.1 and 1.0 for the neutral and anionic systems, respectively. Thus we find, computationally, that the neutral catalyst is 2.1 times slower than the anionic system, in fair agreement with experimental results.

We shall now turn to our second objective, the discussion of the catalyst poisoning after the first AN insertion.

Isomerization and Chelate Formation after a Prior 2,1 Acrylonitrile Insertion. The 2,1 insertion of the acrylonitrile into an M−P bond leads to an α-cyano complex, as it is shown in Schemes 5 and 10. The cyano group is able to form a stable four member chelate ring with the metal atom. The stability of the α-cyano chelate depends on the electrophilic nature of the central atom. For cationic palladium Brookhart systems the Pd(II)−N bond is much stronger than that for the neutral systems.[20] For a neutral system like complex **1** where the BF_3^- anionic substituent is close to the metal center, its fluorine atom binds strongly to the nickel atom causing a competition with the CN group. Therefore the four member chelate structure is only more stable than the nonchelated complex **1**/**J** by 4.1 kcal mol^{-1}. H-agostic complexes on the other hand are thermodynamically less stable than the complexes without an H-agostic bond by 1.7 kcal mol^{-1}. This is in contrast to the cationic or backbone substituted neutral complexes where the N-chelated complexes are much more stable than the nonchelated or H-agostic conformations. The difference is again attributed to the destabilizing influence of the anionic substituent in the ortho position of the aryl ring on the Pd−N chelating bond.

Four or five member cyano-chelate complexes can be formed by chain walking involving a H-transfer reaction, as illustrated in Scheme 10. None of the products of the H-transfer isomerization reactions give rise to chelating isomers with a higher thermodynamic stability than the α-CN-chelate complex. The energies of the five- and six-member CN chelateing complexes are higher than the α-chelated cyano isomer by 4.3 and 4.9 kcal mol^{-1}, respectively, Scheme 10. The barrier for the chain walking isomerization reactions is fairly high (∼16 kcal mol^{-1}). Therefore higher member chelate formation is both kinetically and thermodynamically disfavored over uptake of the next monomer and are thus not likely to poison the catalyst.

Catalyst Dimerization and Trimerization Reactions after the Monomer Insertion. In recent experimental studies, stable oligomer formation of the catalyst itself has been observed, using neutral Grubbs-type Pd−N^O complexes or cationic Brookhart-type Pd−N^N catalysts, after the first 2,1 acrylonitrile insertion.[17,18] The dimers and trimers formed after the first AN insertion are very stable, and although they can be broken up with strong donors such as PMe_3, they are unreactive toward ethylene or acrylonitrile, thus giving rise to a thermodynamic sink in the cycle. These observations were also supported by theoretical calculations due to Yang et al. for the neutral Pd−N^O systems **12** and **13**.[20]

To avoid the oligomerization of the active species, the dimer (**P**) or trimer (**Q**) must be thermodynamically less favored than the formation of the N- or π-complex (**M**, **N**, **O**) after the next ethylene or acrylonitrile uptake (Scheme 5). In the following we shall investigate oligomerization vs acrylonitrile coordination by N-complexation for the neutral nickel and palladium Brookhart diimine complexes. Once oligomer formation is unfavored against π- or N-complex formation, even with a moderately poisoned system, the $\pi-\sigma$ equilibrium can produce a π-complex which can undergo an insertion reaction. The relative stabilization energies for the competitive oligomerization and N-complexation reactions, with respect to the 2,1 acrylonitrile insertion product **F**, are shown in Table 4 and illustrated in Scheme 11.

The ortho aryl substitution motif in complex **1** shows great promise in terms of increased functional group tolerance, since it weakens primarily the Ni−N(cyano) bond. This can already be seen on the remarkable π- vs σ-complexation energy of acrylonitrile.[19] The next monomer uptake with N-complexation of an ortho aryl BF_3^- nickel complex, **1**/**F**→**1**/**O**, is remarkably competitive with the formation of oligomers, **1**/**F**→**1**/**P** or **1**/**F**→**1**/**Q**. One may rationalize this behavior with the presence of the BF_3^- anionic group close to the metal center. Based on the direct Ni−F_3B^- contact, similar to the acrylonitrile N-coordination, the N-binding of the adjacent α-cyano-alkyl groups

Scheme 10. Isomerization by H-Transfer Reaction after 2,1 Acrylonitrile Insertion[a]

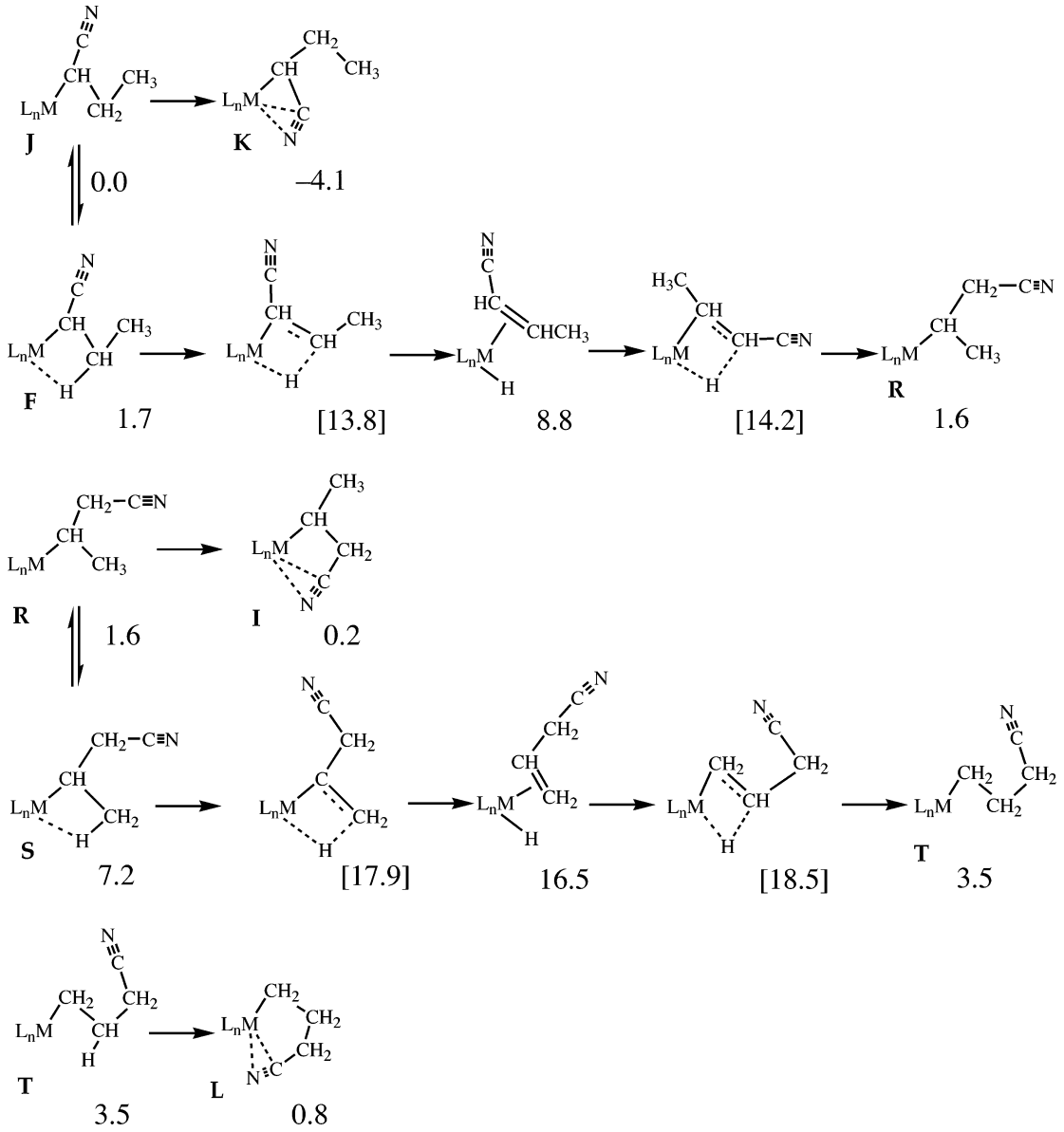

[a] Relative energies, in kcal mol^{-1}, are shown with respect to complex **1**/**J**. Isomerization barriers are shown in parentheses in kcal mol^{-1}.

Table 4. A Comparison between AN Complexation Energies to Catalyst Unit and Catalyst Di- and Trimerization Energies Per Unit

ID	N-complex $\Delta H(\mathbf{O})^{a,b}$	dimer $\Delta H(\mathbf{P})^{a,c}$	trimer $\Delta H(\mathbf{Q})^{a,d}$	N-complex $\Delta G(\mathbf{O})^{a,e,h}$	dimer $\Delta G(\mathbf{P})^{a,f,h}$	trimer $\Delta G(\mathbf{Q})^{a,g,h}$
1	−22.8	−9.3	−17.4	−13.8	−0.2	−11.4
10	−18.0	−13.2	−20.8	−9.0	−8.7	−14.8
9	−25.4	−27.3	−29.6	−16.4	−15.2	−23.6
11	−23.9	−25.7	−32.1	−14.9	−21.2	−26.1

[a] For definitions of **O**, **P**, and **Q** see Scheme 11. [b] The enthalpy of AN complexation to one catalyst unit, see Scheme 11. [c] The enthalpy per unit for catalyst dimerization. [d] The enthalpy per unit for catalyst trimerization. [e] The free energy of AN complexation to one catalyst unit, see Scheme 11. [f] The free energy change per unit for catalyst dimerization. [g] The free energy change per unit for catalyst trimerization. [h] The entropic contribution $-T\Delta S$ to the free energies was taken as 9 kcal mol^{-1} per catalyst unit.

is weakened. However, we note that the Brookhart-type N^N catalyst is considerably bulkier than the Grubbs-type N^O complex, since it contains two bulky 2,6-diisopropyl-phenyl side groups in contrast with the N^O systems, which contains only one bulky side group. Therefore we have also studied the palladium(II) and nickel(II) backbone substituted complexes with two bulky side groups.

The data in Table 4 show that for the Ni(II) complex **1** the N-complex formation, $\Delta G(\mathbf{O})$, is favored over trimerization, $\Delta G(\mathbf{Q})$. For the Pd(II) complex the trimer formation, $\Delta G(\mathbf{Q})$, is still preferred by 6 kcal mol^{-1}; however the dimer formation, $\Delta G(\mathbf{P})$, is comparable with the N-complexation, $\Delta G(\mathbf{Q})$, in stability.

We have also looked at the competition between N-complex formation and catalyst oligomerization for the Ni(II), **9**, and Pd(II), **11**, Brookhart systems where the anionic substitution in terms of BH_3^- is introduced at the backbone of the diimine ring where it cannot directly interact with the metal center. For both systems there is a clear preference for trimerization, $\Delta G(\mathbf{Q})$, over N-complexation, $\Delta G(\mathbf{O})$. It is clear that the anionic group must be able to interact with the metal center in order to prevent oligomerization as in **1**.

Scheme 11. Oligomerization vs N-Complexation Reaction, with ΔH Values Shown for Complex **1**

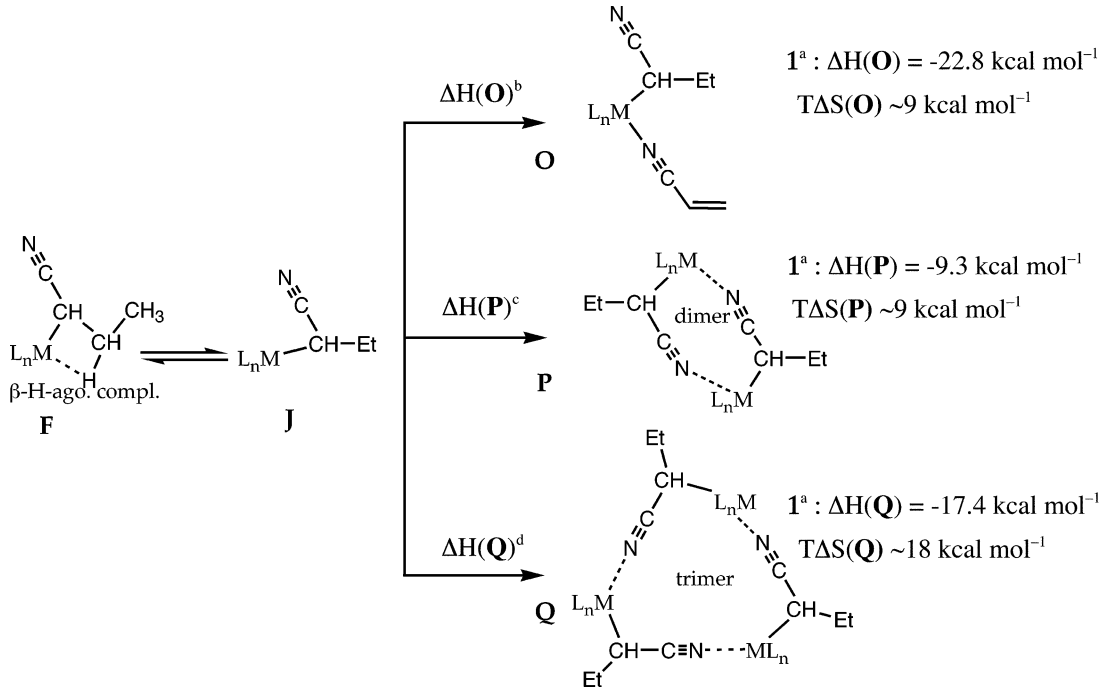

[a] For enthalpy values for other catalysts and corresponding free energy values, see Table 4. [b]The enthalpy of AN complexation to one catalyst unit. [c]The enthalpy per unit for catalyst dimerization. [d]The enthalpy per unit for catalyst trimerization.

We finally suggest that the introduction of a BF_3^- group into the aryl ring of the Grubbs system, rather than at the backbone, might prevent oligomerization of this catalyst as well.

Conclusions

It is a prerequisite for a good polar copolymerization catalyst that the π-complexation be at least competitive in strength with the σ-binding, so that the catalyst is not poisoned. However, a good ethylene propagating polymerization catalyst should have a low barrier of insertion and a strong π-complexation. The overall propagation rate of acrylonitrile should be close to the corresponding propagation rate of ethylene, and the catalyst should have a low affinity toward side reactions, such as chelate formation and catalyst oligomer formation after the acrylonitrile insertion.

Based on the presented kinetic model for propagation we were able to rank the various diimine-based catalyst candidates. The efficiency of a catalyst candidate is measured in terms of the log of the relative rate of propagation, $\log(k_{rel})$ and $\log(k'_{rel})$, for ethylene and acrylonitrile, respectively, with respect to the cationic Brookhart catalyst. The calculated relative propagation rates for acrylonitrile insertion are in good agreement with Piers' experimental measurements (presented herein).

In terms of the relative propagation rate the best catalyst candidates for copolymerization of ethylene and acrylonitrile are complexes **1**, **4**, **6**, **7**, and **9**. Complex **9** can insert ethylene only 10^1 times slower than the cationic Ni−Brookhart catalyst, while complex **6** can insert acrylonitrile about 10^3 times slower, with both being superior in functional group tolerance compared to the original cationic Brookhart catalyst. The presented kinetic model is based on monomer concentration estimates that are identical for ethylene and acrylonitrile. Since experimental polar copolymerization reactions are run with an excess of acrylonitrile relative to ethylene, these results are even more promising given that one can easily use a greater concentration of acrylonitrile.

In the second part of our study, for the neutral catalyst **1** we illustrate that none of the products of the H-transfer isomerization reactions give rise to chelating isomers with a higher thermodynamic stability than the α-CN-chelate complex. The barrier of these reactions is fairly high and are not competitive with the next monomer uptake.

Catalyst oligomerization reactions can be disfavored inserting the BF_3^- anionic substituent into the aryl group at the ortho position of the neutral nickel diimine complex (**1** and **6**). The anionic group at the front side of the catalyst is able to establish a direct contact to the metal center and thus destabilize the oligomers. We also demonstrated that the substitution on the catalyst backbone (**9**) does not destabilize the dimer or trimer structures to the same degree.

Furthermore we propose that the experimentally observed oligomerization reactions after the first acrylonitrile insertion for N^O type complexes can also be eliminated by using anionic substitution at the ortho position of the aryl group.

Acknowledgment. An important part of the calculations has been performed by WestGrid computers. This work has been supported by the National Sciences and Engineering Research Council of Canada (NSERC), as well as Bayer Material Science and Lanxess. T.Z. thanks the Canadian government for a Canada Research Chair.

Supporting Information Available: Geometries of transition states for compounds **1**−**11** and geometries of stationary points for compounds **9**−**11**. Graphical representations of relative rates of ethylene and acrylonitrile propagation into M−P bond (M = Ni/Pd, P = Me/Propyl/CH(CN)Et). Geometries of stationary points and transition states for isomerization and oligomerization reactions. This material is available free of charge via the Internet at http://pubs.acs.org.

JA052350X